Sol-gel mesoporous phosphate-based glasses for bone tissue engineering applications

F. Foroutan,[a] I. Abrahams,[b] B. A. Kyffin,[a] A. Corrias,[c] P. Gupta,[d] B. E. Velliou,[d] J. C. Knowles,[e,f,g,h] D. Carta[a,]*

[a] *Department of Chemistry, University of Surrey, GU2 7XH, Guildford, UK.*

[b] *Materials Research Institute, School of Biological and Chemical Sciences, Queen Mary, University of London, Mile End Road, London E1 4NS, UK.*

[c] *School of Physical Sciences, University of Kent, Canterbury, CT2 7NH, UK.*

[d] *Department of Chemical and Process Engineering, Bioprocess and Biochemical Engineering group (BioProChem), University of Surrey, Guildford, UK.*

[e] *Division of Biomaterials and Tissue Engineering, University College London, Eastman Dental Institute, 256 Gray's Inn Road, London WC1X 8LD, UK.*

[f] *The Discoveries Centre for Regenerative and Precision Medicine, UCL Campus, London, UK.*

[g] *Department of Nanobiomedical Science & BK21 PLUS NBM Global Research Center for Regenerative Medicine, Dankook University, Cheonan 31114, Republic of Korea.*

[h] *UCL Eastman-Korea Dental Medicine Innovation Centre, Dankook University, Cheonan 31114, Republic of Korea.*

**Corresponding author: Dr D. Carta, Department of Chemistry, University of Surrey, GU2 7XH, Guildford, UK. Email: d.carta@surrey.ac.uk*

Abstract

In the present study, mesoporous phosphate-based glasses (MPGs) in the P_2O_5-CaO-Na_2O system were synthesised, for the first time, using a combination of sol-gel chemistry and supramolecular templating. By using the non-ionic triblock copolymer Pluronic 123 (P123) as a structure-directing agent, an extensive network of channel-like pores of around 12 nm and surface area of 124 $m^2.g^{-1}$ was obtained. Investigation of phosphorus, calcium, and sodium release in deionised water over time has shown that MPGs have great potential as bioresorbable controlled delivery system. A comparison between the structural properties, bioactivity and biocompatibility of the MPGs with non-porous phosphate-based glass (PGs) of analogous composition was performed. Results indicate that MPGs have enhanced bioactivity and biocompatibility compared to PGs despite having similar local structure and dissolution properties. Differently from PGs, MPGs show formation of hydroxyl carbonate apatite (HCA) on their surface after 24 hours of immersion in simulated body fluid. Moreover, MPGs show enhanced viability of Saos-2 osteosarcoma cell after 7 days of culturing. This suggests that textural properties (porosity and surface area) play a crucial role in the kinetic of HCA formation and in interaction with cells. Increased efficiency of drug loading and release over non-porous PGs systems was proved using the antimicrobial tetracycline hydrochloride as a drug model. This study represents a significant advance in the field of mesoporous materials for drug delivery and bone tissue regeneration as it reports, for the first time, the synthesis, structural characterisation and biocompatibility of mesoporous amorphous calcium phosphate glasses.

Keywords: Mesoporous materials, phosphate glasses, bone regeneration, drug delivery.

1. Introduction

Mesoporous glasses for biomedical applications have gained increasing attention in the past years. [1] [2] [3] Their main characteristics are the presence of extended porosity with pores in the size range of 2-50 nm, high surface areas and high pore volumes which make them ideal systems for controlled drug delivery and tissue regeneration applications. Introduction of mesoporosity into biomedical glasses i) enhances the interaction between the bioresorbable implant and the physiological fluids; ii) facilitates the absorption and delivery of therapeutic molecules thanks to the open porous structure and homogeneity of pore sizes; iii) guarantees multifunctionality, by combining drug delivery and cell stimulation. Up to date, a significant amount of work has been performed on the synthesis of mesoporous silicate-based glasses mainly as drug delivery systems [4] [5] and for bone tissue regeneration applications.[6] It has been shown that mesopores can be loaded with high dosages of osteogenic agents and therapeutic molecules and that high surface areas enhance the bioactivity of silicate-based glasses. [7] [8] However, to date, there are no examples of mesoporous phosphate-based glasses (MPGs) reported in literature. The synthesis of MPGs has been considered in a recent review as "*a significantly challenging area for future efforts"*. [8] This is because the phophate-based glass network is more prone to collapsing and crystallisation than the silicate-based glasses under the processes required to obtain the mesoporous structure. [8] It has also to be noted that the synthesis of mesoporous oxides containing P and Ca is particularly challenging even in crystalline form. [9]

Phosphate-based glasses (PGs) have recently been presented as a promising new generation of biomaterials alternative to the silicate-based glasses. Differently from the silicate-based, phosphate-based glasses are bioresorbable as they react and dissolve in the physiological environment and they are eventually totally replaced by regenerated hard or soft tissue. [10] [11][12][13] Therefore, PGs present a great advantage over silicate-based glasses which have a

very slow solubility and can only be used to manufacture long-term implants which are susceptible of long-term failure/inflammatory reactions. Thanks to their complete solubility with degradation products that can be easily metabolised in the body, PGs can be used as safe degradable temporary implants, avoiding the necessity of a secondary operation for their surgical removal. [10] Moreover, PGs can be used as controlled local delivery systems of therapeutic molecules (*e.g.* antimicrobial ions/growth factors) that will be slowly released as the implant degrades. *In situ* controlled delivery avoids the need for oral administration and injection, improving the quality of life of patients. As the ions released from PGs already exist in the body, low toxicity and good biocompatibility is guaranteed.[14]

Mesoporous materials are usually prepared in solution via supramolecular chemistry using surfactants, which templates the inorganic material. Surfactants spontaneously organise (self-assemble) in specific-shaped micelles at the critical micellar concentration, the shape and size depending on the specific surfactant used.[3] After removal of the surfactant via calcination or solvent exchange, pores having the sizes of the micelles are left in the inorganic material. The conventional melt-quench method (MQ) of preparing PGs cannot be used for the synthesis of MPGs because it requires melting of oxide powders at temperatures >1100 °C and rapid cooling.[15] Moreover, this method often leads to non-homogeneous, bulk glasses that cannot be used for hosting temperature sensitive molecules. [16]

The sol-gel process (SG), a wet chemical bottom-up technique based on the hydrolysis and polycondensation of precursors in solution, has been found an excellent alternative synthetic route to MQ for the production of PGs.[8][17][18][19] In particular, the SG process is ideal for the synthesis of mesoporous systems. Surfactant molecules can be easily added using the SG method into the precursor's solutions and the morphology of pores can be tailored thanks to the easily controlled solution-based chemistry.

Silicate-based glasses in the SiO_2-CaO-Na_2O-P_2O_5 system synthesised via the SG method have shown to bond to the living bone through the formation of a hydroxyl carbonate apatite (HCA) layer on their surface.[20] It has been shown that the much higher porosity and surface area inferred by mesopores enhances the bioactivity of silicate-based sol-gel glasses by accelerating the rate of HCA formation and providing an ideal support for cell growth and supply of nutrients. [21][22][23] Giving that the composition of PGs is much more similar to the bone/teeth composition than silicate-based glasses, [10] MPGs are expected to induce HCA formation on their surface. As observed in silicate-based glasses, introduction of mesoporosity into the PGs is expected to accelerate the kinetic deposition process of HCA that favouring a process of bone formation.[3]

Mesoporous silicate-based glasses have been used to host, protect and deliver drug molecules to the target site. [24] Recent studies have shown high dosage of antimicrobial drug molecules can be loaded into the mesoporous silicate-based glasses to deliver appropriate drug concentration to the site of infection with minimum side effect to the rest of body. [24][25] Introduction of mesoporosity into PGs would enhance the great potential applications of these materials as controlled drug delivery systems as the majority of drugs used in clinical practise can easily be hosted into the mesopores. [5]

Moreover, similar to the mesoporous silicate-based glasses, the surface of MPGs can be functionalised to avoid burst release and delivering drug molecules to the specific site of action.[26][27]

The present study presents the first example of calcium-based MPGs ever reported and investigates their potential applications as multifunctional materials for controlled drug delivery and bone tissue regeneration. The structure of MPGs was analysed using several complementary characterisation techniques such as wide and low angle X-ray diffraction (WA-

XRD and LA-XRD), ^{31}P solid-state magic angle spinning nuclear magnetic resonance (^{31}P MAS NMR), Fourier transform infrared spectroscopy (FT-IR), scanning electron microscopy (SEM) and Energy dispersive X-ray analysis (EDX). Pore morphology and surface area were investigated using N_2 absorption at 77 K, and their degradation over time was monitored via inductively coupled plasma-optical emission spectroscopy (ICP-OES). Biocompatibility was assessed by *in vitro* culturing of Saos-2 osteoblast-like cells. Drug loading efficiency and controlled release was investigated by incorporating into the MPGs system tetracycline hydrochloride (TCH), a commonly used broad spectrum antibiotic that inhibits protein synthesis. [28] A comparison between a mesoporous glass and non-porous glass of the same composition prepared via the same sol-gel synthesis method but in absence of templating surfactant is presented.

2. Materials and methods

2.1. Materials

The following chemicals were used without further purification: n-butyl phosphate (1:1 molar ratio of mono $OP(OH)_2(OBu)$ and di-butyl phosphate $OP(OH)(OBu)_2$, Alfa Aesar, 98%), calcium methoxyethoxide (Ca-methoxyethoxide, abcr, 20% in methoxyethanol), sodium methoxide solution (NaOMe, Aldrich, 30 wt% in methanol), ethanol (EtOH, Fisher, 99%), and Pluronic (P123, M_n=5800, Aldrich).

2.2. Synthesis method

n-butyl phosphate was diluted in EtOH (molar ratio 1:3) in a dried vessel and left for 10 minutes. Ca-methoxyethoxide and NaOMe were then added dropwise into the mixture while stirring; the solution was kept under stirring for about 1 h. The mixture was then divided into two parts: one was used to obtain mesoporous phosphate-based glasses (MPGs) and the other

was used to prepare non-porous phosphate-based glasses (PGs) for comparison purposes. In order to prepare the MPGs, P123 dissolved in EtOH and then water added to the mixture (P123: EtOH: H_2O molar ratio 0.05:2:1) before adding to the initial mixture and allowed to react for 10 min. For the preparation of PGs, the initial mixture was used without any addition. PGs and MPGs mixtures were then poured into glass containers and allowed to gel at room temperature. Both mixtures turned to gel after about 10 minutes and they were aged for 1 day at room temperature. Gels were then dried using a multi-step drying ramp: the temperature was increased from room temperature to 40 ˚C and held for 1 day, then to 60 ˚C and held for 2 days, then to 80˚C and held for 2 days and finally to 120 ˚C and held for 1 day. Then a calcination step was performed by heating the glasses at 300 ˚C and held for 1 h to remove the surfactant and any remaining solvents from the sample. A heating rate of 1 ˚C.min^{-1} was used in all steps in order to prevent the collapse of the mesoporous structure. The obtained glasses were ground at 10 Hz to form microparticles (MM301 milling machine, Retsch GmbH, Hope, UK) and microparticles in the size range of 106–200 μm were obtained using test sieves (Endecotts Ltd, London, UK). A flow diagram for the synthesis of MPGs is presented in **Figure 1**.

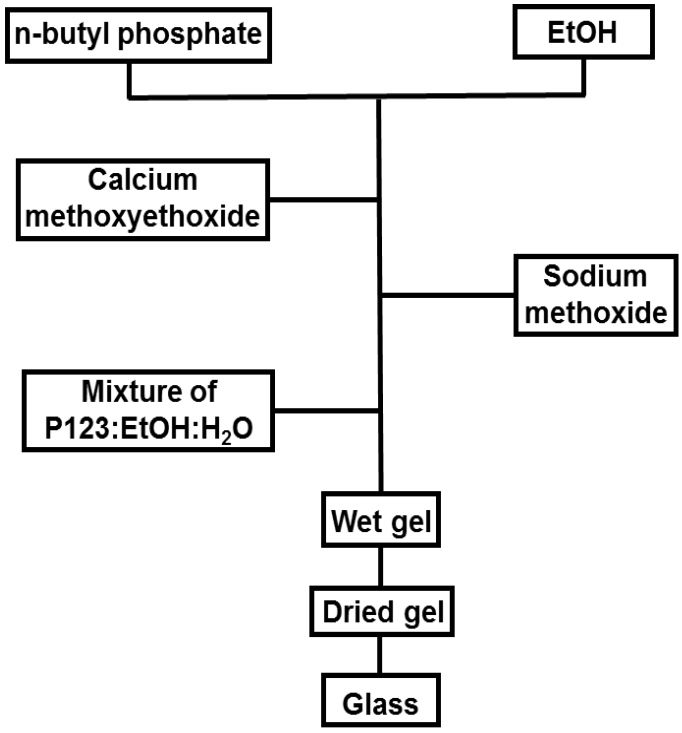

Figure 1. Flow diagram for the preparation of MPGs.

2.3. Characterisation

Wide angle X-ray diffraction (WA-XRD, PANalytical X'Pert, Royston, UK) was performed in a flat plate geometry using Ni filtered Cu Kα radiation. Scans were collected using a PIXcel-1D detector with a step size of 0.0525° over an angular range of 2θ =10-90° and a count time of 12 s per step.

Low angle X-ray diffraction (LA-XRD, PANalytical X'Pert, Royston, UK) was performed using Ni filtered Cu Kα radiation in transmission mode using a focusing mirror on the X-ray incident beam. Scans were collected using a PIXcel-3D detector with a step size of 0.0525° over an angular range of 2θ = 0.3–6.0 with a count time per step of 0.017 s.

Scanning electron microscopy (JSM-7100F, Jeol, Welwyn, UK) was performed at an accelerating voltage of 5 kV and working distance of 10.0 mm. The samples were mounted onto an aluminium stub using carbon conductive tape. Image-pro plus software (Media Cybernetics, USA) was used for image analysis. Energy Dispersive X-ray spectroscopy (EDX,

MagnaRay, ThermoFisher, Hemel Hempstead, UK) was performed using an SEM operating at 20 kV, spot size 6 and a working distance of 10 mm.

Solid state ^{31}P MAS NMR spectra (^{31}P MAS-NMR, AVANCE III, Brüker, Coventry, UK) were referenced to the resonance of the secondary reference ammonium dihydrogen phosphate ($NH_4H_2PO_4$) at 0.9 ppm (relative to 85% H_3PO_4 solution at 0 ppm). The spectra was recorded at 161.87 MHz for the loaded powder sample into a 4.0 mm (rotor o.d.) magic angle spinning probe using direct excitation with a 90° pulse and 60 s recycle delay at ambient probe temperature (~ 25 °C) and at a sample spin rate of 12 kHz. Between 20 and 88 repetitions were accumulated and were processed using Dmfit software package.[29]

Fourier Transform Infrared (FT-IR, 2000 series, Perkin Elmer, Seer Green, UK) spectra were acquired with attenuated total reflectance accessory (Golden Gate, Specac, Orpington, UK) using Timebase software (Perkin Elmer). Spectra were collected at room temperature in absorbance mode in the wavenumber range of 1500-600 cm^{-1}.

Surface area, pore size and pore volume were obtained from N_2 adsorption-desorption measurements (Gemini V, Micromeritics, Hertfordshire, UK) at 77 K; in particular, the specific surface area (SSA) was assessed by using the Brunauer-Emmet-Teller (BET) method, whereas the pores size distribution was determined from the desorption branch of the isotherm through the Barrett-Joyner-Halenda (BJH) method. Samples were outgassed at 270 °C for 6 h prior the measurements.

2.4. Dissolution studies and pH changes

Dissolution studies were performed by soaking 10 mg of the MPG and PG powders in 10 mL of deionised water for up to 7 days. Three replicates were performed for each time point (n=3). The resulting suspensions for each time point were centrifuged at 4,800 rpm for 10 min to separate the undissolved samples from the solution. Concentration of phosphorus, calcium, and

sodium in the solution were measured by inductively coupled plasma-optical emission spectroscopy (ICP-OES, 720ES-Varian, Crawley, UK) calibrated across the predicted concentration range using a multi-element standard solution (VWR, Lutterworth, UK). Both samples and standards were diluted in 1:1 in 4% HNO_3 (Fluka) and analysed in reference to a blank solution (2% HNO_3) under standard operating conditions (Power: 1350 W; Coolant Flow: 15.0 $L.min^{-1}$: Axillary Flow: 1.0 $L.min^{-1}$).

Changes of pH over time were investigated by soaking 10 mg of the MPG and PG powders in 10 mL of deionised water (pH= 7.0 ± 0.1) and cell culture medium (pH= 7.8± 0.1). The solutions stored at 37 °C and the pH was measured for up to 7 days with three replicate for each time point using an Orion pH meter (Thermo scientific-Orion star, Loughborough, UK).

2.5. *In vitro* bioactivity and biocompatibility assessment

In vitro bioactivity was evaluated by immersing 25 mg of MPG and PG powders in 25 mL of simulated body fluid (SBF), a solution with ion concentrations very similar to human blood plasma,[30] stored in an incubator at 37 °C while shaking at 100 rpm for 24 h. The samples then washed with water and ethanol and finally dried at 60 °C for 6 h before WA-XRD characterisation and observation of their surfaces with SEM.

In vitro biocompatibility was assessed by seeding Saos-2 cells (HTB85, ATCC, UK) on MPG and PG powders. Saos-2 cells were chosen as representative of osteoblast behaviour and cultured in medium (McCoy's 5a, ATCC, UK) with 15% fetal bovine serum (FBS, Gibco, Invitrogen, Loughborough, UK) and 1% Antibiotic-Antimycotic (Thermo Scientific, Loughborough, UK) in a humidified incubator at 37 °C and 5% CO_2. On reaching 90% confluency, cells were passaged and used for cytocompatibility analysis. To facilitate the attachment of the cells on to the MPG and PG powders for SEM imaging, polycarbonate cell culture inserts with 0.4 μm pore size (Millipore, Merck, UK) were used. 10 mg of MPG and

PG powders were placed on the inserts and incubated with the medium overnight. 1.2 x10^4 cells were placed in each insert and cultured for 7 days with cell viability assessment during the culture period. Cells only on inserts were used as a control for comparison purposes.

SEM was used to visualise cell attachment and growth on MPG and PG surfaces. At the end of day 7, cells were fixed with 3% glutaraldehyde (Sigma-Aldrich) followed by dehydration using graded ethanol. Samples were then air dried, gold sputter coated and visualised using SEM. To visualise the nucleus and actin filaments, cells were fixed using 4% paraformaldehyde and stained with DAPI- Phalloidin at the end of day 7. Samples were incubated for 20 mins at room temperature in staining solution containing 2.5 µL of DAPI (1 mg.mL^{-1} stock solution), 4 µL of Phalloidin (200 U.mL^{-1} stock concentration, Alexa Fluor 488, Phalloidin, Life Technologies) and 20 µL of Triton X per mL of PBS. Cells were then visualised using cell image multi-mode reader (Cytation-5, BioTek, Swindon, UK).

2.6. Drug loading and *in vitro* drug release study

To assess the intake of drugs for controlled delivery applications of MPGs and PGs, the tetracycline hydrochloride (TCH) was added to both samples via impregnation. 5 mg of MPG and PG powders were soaked in 5 mL TCH solution prepared by adding 5 mg TCH in 5 mL of ethanol. The mixtures were stirred for 60 min at room temperature and then centrifuged at 4,800 rpm for 5 min to separate the impregnated glass particles from the solutions. The glasses impregnated with TCH were then washed once with ethanol and centrifuged to remove the excess of unloaded TCH. The glasses were then dried overnight at room temperature. TCH release was assessed by adding 5 mL of deionised water to the samples, keeping them in an incubator at 37 °C under shaking at 100 rpm and collecting the solution at different time points up to 24 h. Three replicates for each time point were measured.

TCH release was assessed via UV–Vis absorption (Libra, BioChrom, Cambridge, UK) in the range of 300 - 500 nm wavelength (step size 1 nm). Deionised water was used as a blank and calibration curve for TCH standard solutions in deionised water was plotted in the range of 0.1-1000 $\mu g.mL^{-1}$.

3. Results and discussion

Chemical analysis of MPG and PG was carried out using SEM equipped with an EDX detector in order to determine their exact composition. **Table 1** reports **c**ompositions expressed in terms of oxide mol %; Elemental compositions in terms of weight % and mol % along with the EDX spectra are reported in **Table S1** and **Figure S1**, respectively.

As expected, MPG and PG have very similar composition (P_2O_5 ~ 45-46 mol%, CaO ~ 35-36 mol % and Na_2O ~ 19 mol %). The oxides content was chosen on the basis of previous studies on MQ and SG phosphate-based glasses. Glasses with P_2O_5 content in the range 40-50 mol % and CaO content in the range 20-40 mol % have been shown to have good bioactivity and biocompatibility.[17] [31] [32]

Table 1. Compositions of MPG and PG measured by EDX.

Glass Code	**Oxides (mol %)**		
	P_2O_5	**CaO**	**Na_2O**
MPG	45.0 (±1.2)	36.0 (±0.9)	19.0 (±0.5)
PG	46.0 (±0.9)	35.0 (±0.7)	19.0 (±0.6)

In order to assess the amorphous nature of synthesised samples, WA-XRD was performed. The WA-XRD patterns, reported in **Figure 2A**, do not show any Bragg peaks clearly indicating that

both samples are fully amorphous. The only feature observed is a broad halo centred at around 2θ = 28 ° which is due to the amorphous phosphate network. Despite similar content and WA-XRD patterns, MPG and PG are expected to show very different textural properties given that only MPG was synthesised using the templating agent P123. This was confirmed by N_2 adsorption and desorption analysis at 77 K (**Figure 2B**). MPG shows an adsorption-desorption isotherm that can be classified as type IV which is characteristic of a mesoporous materials, whereas PG is clearly non-porous as it does not show any adsorption-desorption isotherm. The shape of the MPG hysteresis loop can be classified as type H1 which is typical of cylindrical pores arranged in a hexagonal manner open at both ends. [22] The presence of cylindrical pores is in agreement with the type of surfactant used (P123) which is known to form cylindrical micelles which aggregate forming two dimensional hexagonal arrangements.[3] The arrays of unidirectional channels of pores distributed in a hexagonal arrangement are formed by removing the surfactant via calcination. MPG presents a narrow, single modal pore size distribution centred at around 12 nm (inset of **Figure 2B**). The surface area calculated using the BET model is 124 $m^2.g^{-1}$ and the pore volume is 0.28 $cm^3.g^{-1}$. Despite the surface area being lower than the typical mesoporous silicate-based glasses, the result is remarkable as it is the first example ever reported of mesoporous calcium phosphate-based glasses which are known to have a much weaker network structure than silicate-based ones.[8] Size of mesopores is also ideal as 12 nm pores can easily accommodate the majority of drug molecules of interest in clinical applications.[7] Further evidence of the presence of mesopores in MPG was given by SEM analysis. The SEM image reported in **Figure 2C** clearly shows a highly porous structure with a pore size range 10-20 nm in good agreement with the pore size distribution obtained via N_2 adsorption at 77 K. A wall thickness of 4-5 nm was estimated from SEM images which is in agreement with typical values found on mesoporous silicate-based glasses prepared using P123 as a surfactant.[33] Moreover, by looking carefully at the local arrangement of pores, a

hexagonal arrangement of mesopores can be seen (zoomed area in **Figure 2C**), suggesting a certain local order of mesopores. This is in agreement with the type H1 hysteresis loop observed in the N_2 adsorption- desorption isotherm, typical of hexagonally ordered mesopores. In order to further investigate the arrangement of mesopores in MPG, LA-XRD was performed on MPG and on PG as a comparison (**Figure 2D**). MPG shows a strong reflection at 2θ = 0.8 ° and a broader reflection at 2θ = 2.6 ° that suggests the presence of a certain order in the arrangement of pores. These reflections could be assigned to the (100) and (200) diffractions of 2D hexagonal mesoporous porous structure, respectively.[9] [34] As expected for a non-porous system, no reflections were observed in the PG sample.

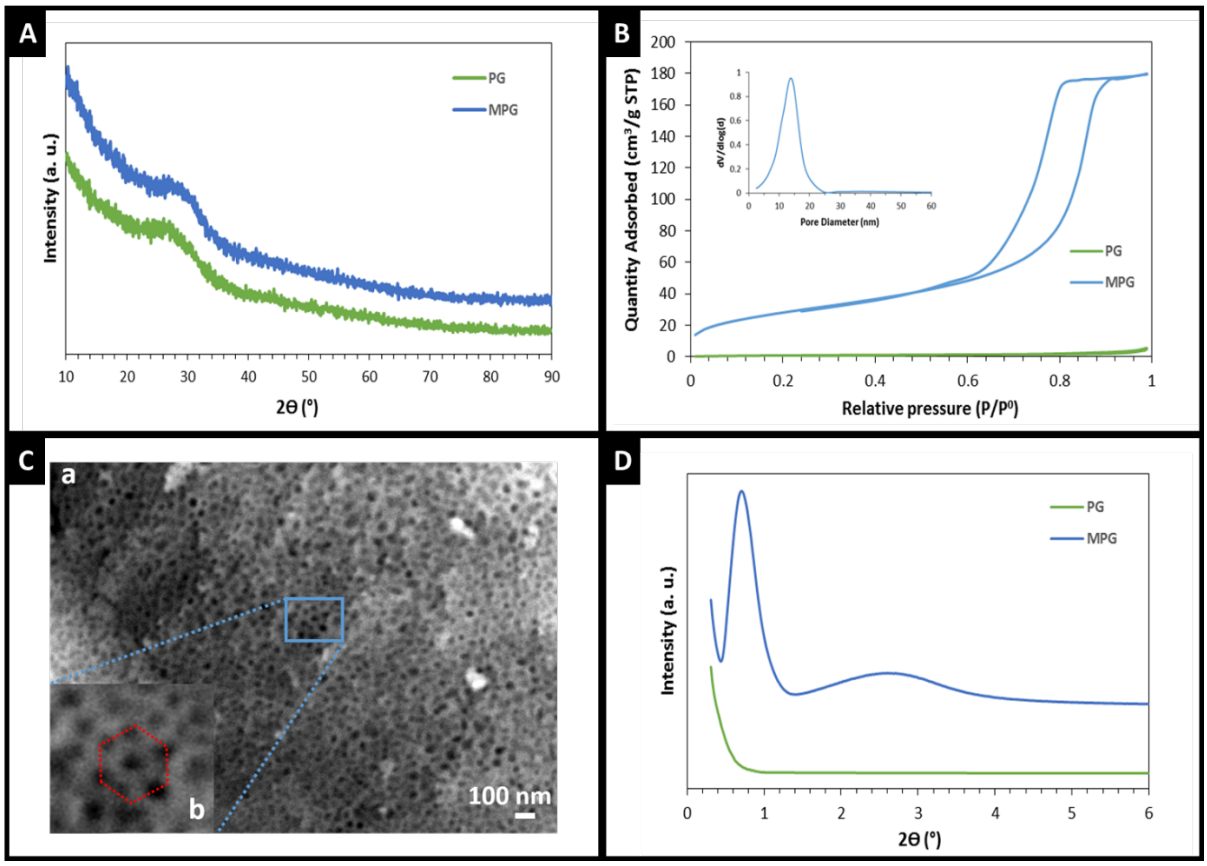

Figure 2. (A) WA-XRD, **(B)** N_2 adsorption and desorption isotherm; Inset: BJH pore size distribution, **(C)** SEM image of MPG **(a)**; detail of blue squared area **(b)**, and **(D)** LA-XRD spectra of MPG and PG samples.

The textural properties of MPGs and PGs are clearly very different as expected. It is therefore interesting to investigate if the different morphologies affect the structural properties, in particular the way the phosphate chains are linked. ^{31}P MAS NMR is a very powerful tool for the investigation of the local environment around phosphorus and the connectivity of the phosphate units. The ^{31}P MAS NMR spectra of both MPG and PG samples are presented in **Figure 3A**. Resonances are assigned to Q^n groups, where n represents the number of bridging oxygens between phosphate units. Relative quantities of Q^n groups were quantified using Dmfit software package. Both spectra show a main resonance at about -6 ppm ascribed to Q^1 groups with relative intensity in the range 68-73% and a less intense resonance (27-32%) at about -23 ppm ascribed to Q^2 groups (**Table S2)**. Results are in agreement with previous studies on non-porous SG phosphate-based glasses of similar composition that show a structure dominated by Q^1 groups with a smaller percentage of Q^2. [14]

A confirmation of the fact that the textural properties do not affect the structure of the phosphate chains is given by FT-IR spectroscopy. As shown in **Figure 3B**, the FT-IR spectra of MPG and PG, measured in the range 600-1500 cm^{-1} are very similar. The band at ~ 1100 cm^{-1} and the shoulder at ~ 1235 cm^{-1} can be assigned to the asymmetric stretching υ_{as} $(PO_3)^{-2}$ and υ_{as} (PO_2) modes, respectively that can be related to Q^1 and Q^2 phosphate units. The band at ~ 900 cm^{-1} and the less intense band at ~730 cm^{-1} can be assigned to the asymmetrical stretching mode υ_{as} (P-O-P) and symmetrical stretching mode υ_s (P-O-P), respectively (Q^2 phosphate units). [19][35]

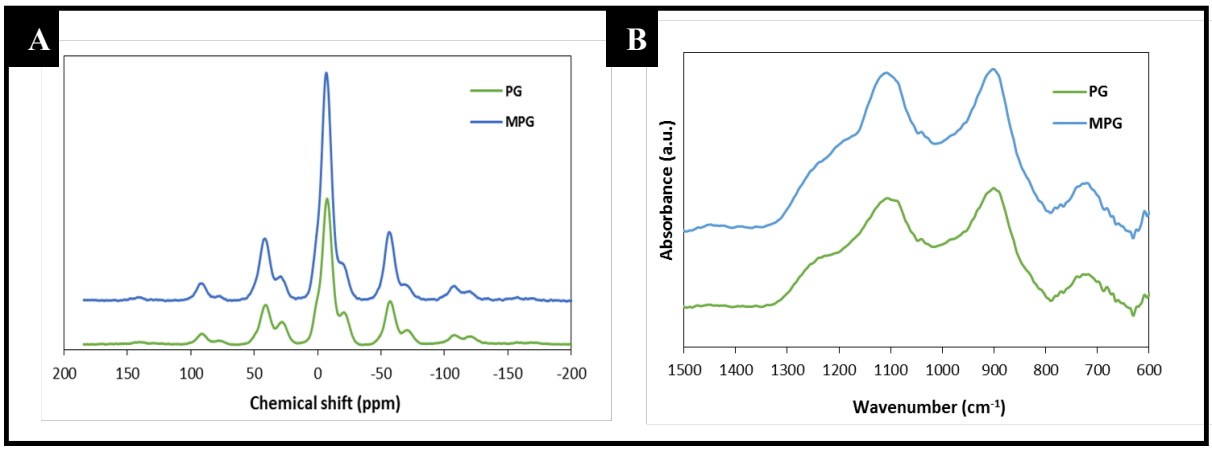

Figure 3. (A) ^{31}P MAS NMR and **(B)** FT-IR spectra of MPG and PG samples.

As phosphate-based glasses have great potential as bioresorbable materials, therefore, dissolution studies are very important to assess their potential as controlled delivery systems. In particular, it is interesting to compare the dissolution properties of MPGs and PGs, given that the two systems have very different textural properties but similar structure. The release of phosphorus, calcium, and sodium in deionised water at different time points up to 7 days was measured via ICP-OES and data presented in **Figure 4A**, **4B** and **4C**, respectively. Results show that release profiles do not change significantly with change in porosity, especially during the first 8 h. In particular, P release is identical in MPG and PG samples for the first 8 h, Ca release is identical for the first 12 h and Na release is identical for the first 72 h. Dissolution trends that follow the initial overlapping release are similar for MPGs and PGs systems. However, a slightly higher amount of P, Ca and Na is released over time by the MPGs system. Along with the dissolution products, pH change was also monitored over time. pH monitoring is important in order to evaluate the potential application of MPGs as biomaterials. Therefore, pH change was monitored in both deionised water and cell culture medium over a period of 7 days **(Figure 4D).** pH changes of MPG and PG samples over time follow a similar trend, as observed for the release of P, Ca and Na. However, pH values for the PG sample are slightly

higher than for MPG. The pH values measured in deionised water remain relatively neutral, dropping from 7.0 to ~ 6.2 after 8 h, increasing slightly up to 24 h and then remaining stable up to 7 days at around 6.4. The pH values measured in cell culture medium drop from 7.8 to 7.4 after 8 h, increasing slightly up to 24 hours and then remaining stable up to 7 days around 7.6. The initial pH reduction can be ascribed to the dissociation of phosphate anions released with formation of phosphoric acid. [36] Following that the slight increase in pH can be related to the presence of Na^+ ions in the solution.

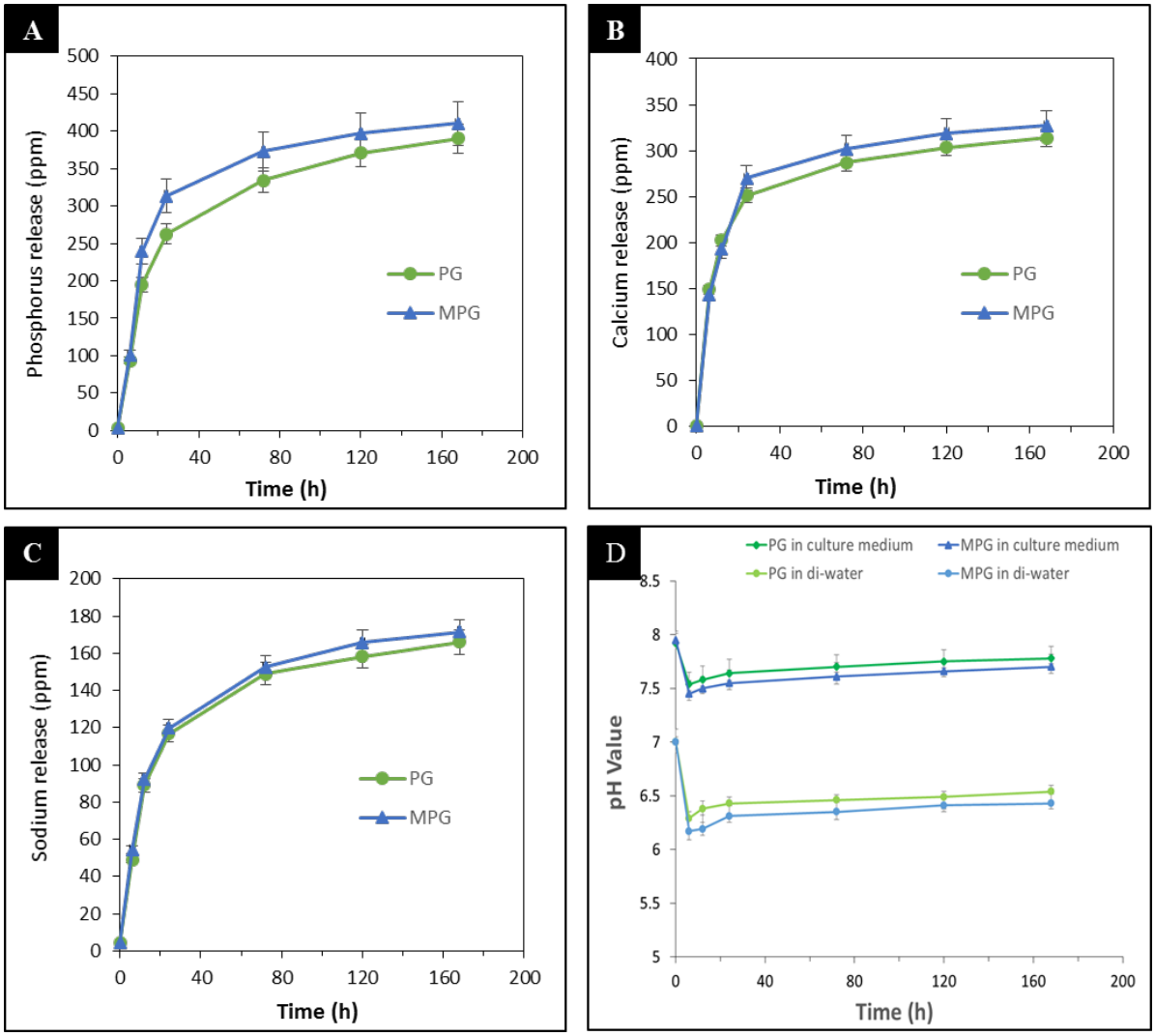

Figure 4. Release of **(A)** phosphorus, **(B)** calcium, and **(C)** sodium in deionised water measured by ICP-OES and **(D)** pH change in deionised water and cell culture medium as a function of time for the MPG and PG samples.

Dissolution studies have shown that P, Ca and Na can be released in a controlled way. The capability of releasing P and Ca ions has been linked to the bioactivity of glasses, in particular with the formation of HCA on the glass surface when in contact with the damaged bone site.[37] As HCA is a naturally occurring mineral present in bones and teeth, the formation of HCA can be used as indication of the bioactivity (osseointegration) of the MPGs.[38] Previous studies have shown that mesoporous silicate-based glasses have superior *in vitro* bioactivity and *in vivo* osteogenic properties compared to the corresponding non-porous systems.[39] However, to the knowledge of the authors, no work has been done on bioactivity of phosphate-based glasses synthesised via sol-gel route.

It is therefore interesting to investigate the capability of MPG and PG in forming HCA on their surface. The *in vitro* bioactivity of the MPG and PG samples was investigated by immersing the glasses in SBF for 24 h. As shown in **Figure 5A**, the WA-XRD pattern of MPG after immersion in SBF clearly indicates the precipitation of a crystalline phase that can be ascribed to HCA (ICDD card No. 24-0033)**.** On the other hand, no crystallisation is observed on the surface of PG. Results are confirmed by SEM analysis that clearly shows formation of HCA nanocrystals only on the surface of MPG but not PG (**Figure 5B and 5C).**

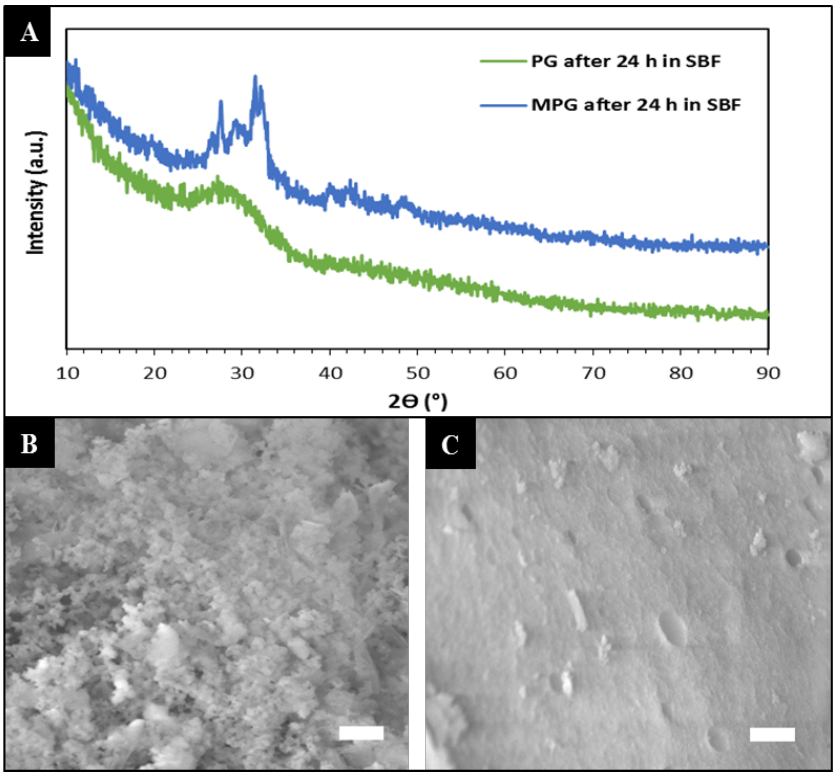

Figure 5. (A) XRD patterns of MPG and PG, SEM images of **(B) M**PG and **(C)** PG after immersion in SBF for 24 h at 37 °C. The scale bar is 1 μm.

It is quite interesting to notice that despite the dissolution studies show that the release of P, Ca and Na is quite similar in MPG and PG, *in vitro* bioactivity has shown formation of HCA only on the surface of MPG after 24 h of immersion in SBF. These results indicate that higher bioactivity can be achieved by solely changing the textural properties of the system. This suggests that high surface area and high porosity allow a better diffusion of physiological fluids into the glass which could be responsible for the enhancement of the kinetic of processes at the interface.[3] Difference in bioactivity cannot be ascribed to a change in the local structure, given that ^{31}P MAS NMR has shown the presence of the same phosphate units (Q^1 and Q^2) in similar amounts and FT-IR spectra are also very similar.

Giving the very promising results on osseointegration of MPG, biocompatibility was assessed by evaluating viability and attachment of Saos-2 osteosarcoma cells cultured on its surfaces. These cells were selected because they possess several osteoblastic features and they can therefore be used to mimic the osteoblast response to the glasses. [40] Saos-2 cells were also cultured on PG for comparison purposes. Control consisted of Saos-2 cells seeded directly on cell culture support.

Cell viability was quantitatively assessed using the Alamar Blue fluorescence assay after 1, 3, 5, and 7 days. The graph shown in **Figure 6A** represents the change in fluorescence of Alamar Blue dye as a direct indicator of cellular metabolic activity which is directly linked to the number of cells. Cell growth does not change significantly in the first 3 days for PG; however MPG shows a slight increase since day 3. At day 5 and 7, both MPG and PG show an increase cell proliferation. However, MPG clearly shows higher cell proliferation than PG.

Cell attachment was assessed via SEM and DAPI- Phalloidin staining. **Figure 6B** shows SEM images of Saos-2 cells nicely attached and well spread on the surface of MPG and PG over a 7-day period. SEM results are confirmed by qualitative analysis based on DAPI- Phalloidin staining (**Figure 6C**). Cells nuclei (blue) and filaments (green) show that cells are attached and spread on MPG and PG surfaces after 7 days of seeding.

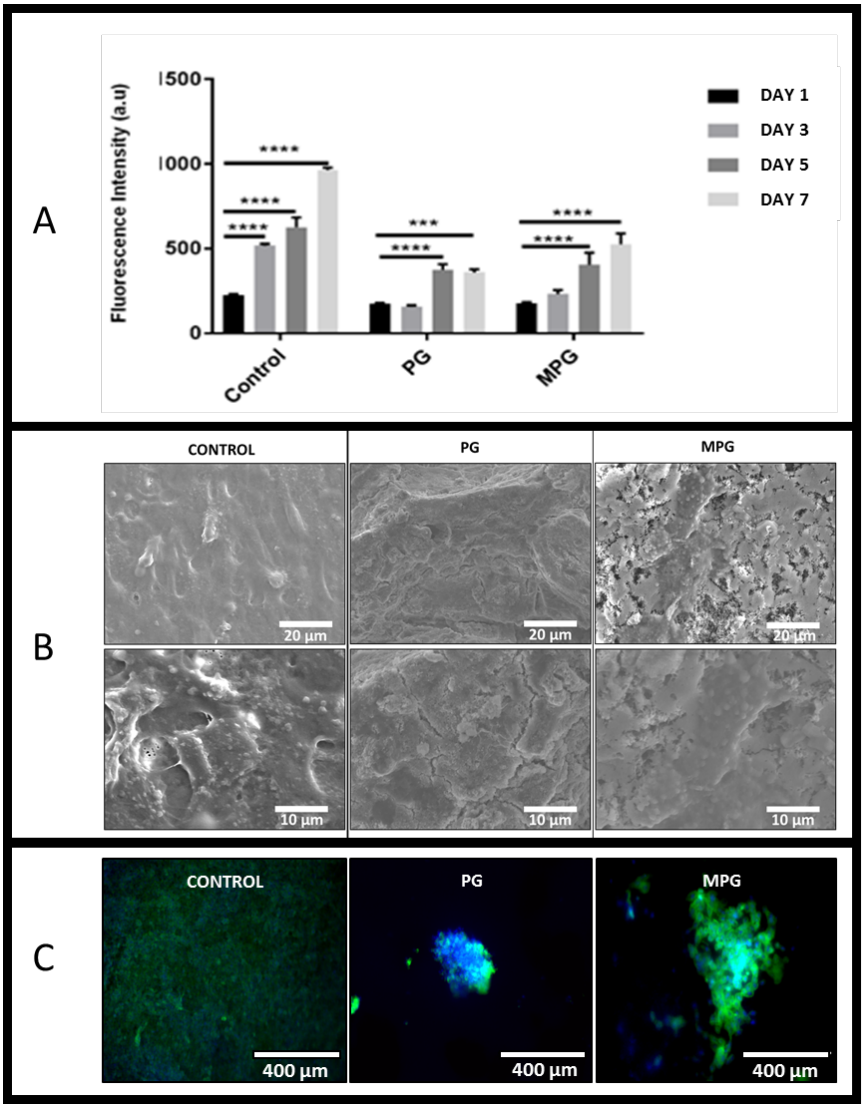

Figure 6. (A) Saos-2 cell viability measurement using the Alamar Blue fluorescence assay after 1, 3, 5 and 7 days; error bars are SD (n=3); **(B)** SEM images showing Saos-2 cells attachment after 7 days at two different magnifications; **(C)** DAPI- Phalloidin staining after 7 days for the MPG and PG samples.

Mesoporous silicate-based glasses have been shown to be excellent drug loading and release systems thank to the extended porosity.[5][24] Therefore, MPG are also expected to show enhanced drug intake and controlled release. This was investigated using tetracycline hydrochloride (TCH) as a model antibiotic often administrated to patient after surgery to avoid bacterial infections. MPG and PG samples were loaded with TCH by impregnation. The release

of TCH in deionised water was then studied over a period of 24 h (**Figure 7**). MPG loaded sample show a sharp TCH release in the first hour (100 μg) followed by a sustained release reaching to 130 μg after 24 h. However, PG loaded sample shows a total release of about 30 μg within the first 30 min. Given that the dissolution properties of the MPG and PG samples in deionised water are very similar, the different TCH release behaviour can be ascribed to a different TCH loading and texture. In particular, the high porosity and surface area of the MPG system allows for a significantly higher drug loading than the non-porous PG which explains the higher release of TCH from MPG loaded sample in comparison with PG. Moreover, MPG shows a more sustained release during the 24 h of the TCH release study. This could be explained considering that TCH molecules are initially incorporated into the mesopores and then slowly released.[41]

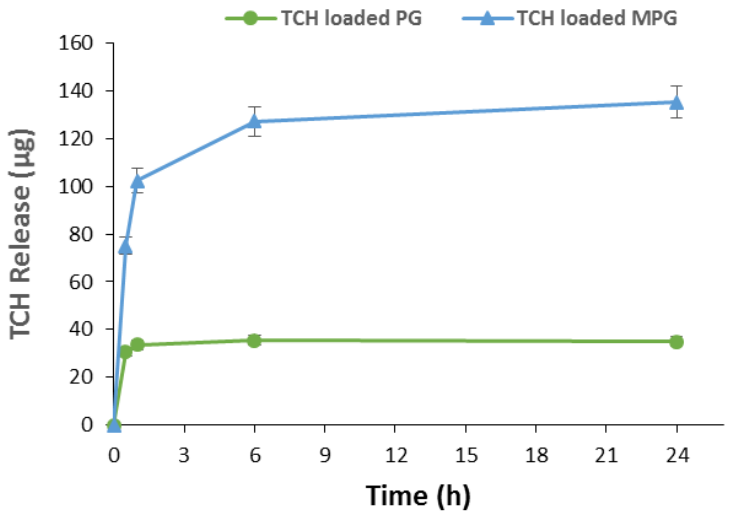

Figure 7. The release profile of TCH as a function of time from MPG and PG loaded samples.

Conclusion

In the present study, mesoporous phosphate-based glasses in the P_2O_5-CaO-Na_2O system were successfully synthesised, for the first time, by using a combination of sol-gel chemistry and supramolecular templating. MPGs have a surface area of 124 $m^2.g^{-1}$, an average pore size of 12 nm, and pore volume of 0.28 $cm^3.g^{-1}$. ^{31}P MAS-NMR shows that they are mainly formed by Q^1 groups (68%) and Q^2 groups (32%). Dissolution studies have shown gradual release of P, Ca and Na over time which makes them excellent candidates as controlled delivery systems. Moreover, pH remains near neutral upon dissolution in cell medium. Despite the fact that MPG and PG have similar structure and dissolution properties, they show very different in vitro bioactivity, biocompatibility and drug loading and release. Mesoporosity has also shown enhancement of kinetic of HCA formation, which appears on the surface of the mesoporous glass within the first 24 h of immersion in SBF. Cytotoxicity studies indicates that mesoporosity enhances Saos-2 osteosarcoma cells attachment and proliferation on the surfaces of the glasses.

Studies on incorporation and release of the antibiotic TCH into MPG have shown that the extended porosity and high surface area allow for a higher loading and more controlled release over time compared to the analogous non-porous system PG.

Results show that the presence of a mesoporous structure clearly enhances bioactivity, biocompatibility, and drug loading capability of the phosphate-based glasses. Therefore, MPGs have the great potential to be used as multifunctional bioresorbable systems, in particular in the field of bone regeneration, by combining formation of new bone tissue with controlled delivery of therapeutic molecules. The novel synthetic route presented in this work opens new horizons in designing a new generation of non- siliceous, mesoporous glasses with great potential in tissue engineering and drug delivery systems.

Supporting Information

Supporting Information is available from the Wiley Online Library or from the authors.

Acknowledgments

The authors would like to acknowledge EPSRC (grant EP/P033636/1) and Royal Society (grant RSG\R1\180191) for providing the funding to conduct this study. The authors are also grateful to Dr David Jones for his help with the SEM/EDX and Dr Graham Palmer for his help with ICP-OES measurements.

Conflict of interest

The authors declare no conflict of interest.

References

[1] Moritz Michal, Malgorzata Geske-Moritz, *Mater. Sci. Eng. C* **2015**, *49*, 114.

[2] C. Wu, J. Chang, *Interface Focus* **2012**, *2*, 292.

[3] I. Izquierdo-barba, O. Access, *Biomed. Glas.* **2015**, *1*, 140.

[4] P. Yang, S. Gai, J. Lin, *Chem Soc Rev* **2012**, *41*, 3679.

[5] M. Vallet-Regí, F. Balas, D. Arcos, *Angew. Chemie - Int. Ed.* **2007**, *46*, 7548.

[6] X. Zhang, D. Zeng, N. Li, J. Wen, X. Jiang, C. Liu, Y. Li, *Sci. Rep.* **2016**, *6*, 19361.

[7] M. Vallet-Regí, *Chem. - A Eur. J.* **2006**, *12*, 5934.

[8] G. J. Owens, R. K. Singh, F. Foroutan, M. Alqaysi, C. M. Han, C. Mahapatra, H. W. Kim, J. C. Knowles, *Prog. Mater. Sci.* **2016**.

[9] B. Tian, X. Liu, B. Tu, C. Yu, J. Fan, L. Wang, S. Xie, G. D. Stucky, D. Zhao, *Nat. Mater.* **2003**, *2*, 159.

[10] J. C. Knowles, *J. Mater. Chem.* **2003**, *13*, 2395.

[11] E. A. Abou Neel, D. M. Pickup, S. P. Valappil, R. J. Newport, J. C. Knowles, *J. Mater. Chem.* **2009**, *19*, 690.

[12] N. Sharmin, C. D. Rudd, *J. Mater. Sci.* **2017**, *52*, 8733.

[13] A. Lapa, M. Cresswell, P. Jackson, A. R. Boccaccini, A. Lapa, M. Cresswell, P. Jackson, A. R. Boccaccini, A. Lapa, M. Cresswell, *Adv. Appl. Ceram.* **2019**, *0*, 1.

[14] F. Foroutan, J. V. Jokerst, S. S. Gambhir, O. Vermesh, H. W. Kim, J. C. Knowles, *ACS Nano* **2015**.

[15] I. Ahmed, M. Lewis, I. Olsen, J. C. Knowles, *Biomaterials* **2004**, *25*, 491.

[16] G. Kaur, G. Pickrell, N. Sriranganathan, V. Kumar, D. Homa, *J. Biomed. Mater. Res. - Part B Appl. Biomater.* **2016**.

[17] D. Carta, D. M. Pickup, J. C. Knowles, M. E. Smith, R. J. Newport, *J. Mater. Chem.* **2005**, *15*, 2134.

[18] D. M. Pickup, P. Guerry, R. M. Moss, J. C. Knowles, M. E. Smith, R. J. Newport, *J. Mater. Chem.* **2007**, *17*, 4777.

[19] F. Foroutan, N. H. de Leeuw, R. A. Martin, G. Palmer, G. J. Owens, H. W. Kim, J. C. Knowles, *J. Sol-Gel Sci. Technol.* **2014**.

[20] T. Kokubo, H. Takadama, *Biomaterials* **2006**, *27*, 2907.

[21] X. Yan, C. Yu, X. Zhou, J. Tang, D. Zhao, *Angew. Chemie - Int. Ed.* **2004**, *43*, 5980.

[22] A. López-Noriega, D. Arcos, I. Izquierdo-Barba, Y. Sakamoto, O. Terasaki, M. Vallet-Regí, *Chem. Mater.* **2006**, *18*, 3137.

[23] Q. H. Shi, J. F. Wang, J. P. Zhang, J. Fan, G. D. Stucky, *Adv. Mater.* **2006**, *18*, 1038.

[24] M. Vallet-Regí, M. Colilla, I. Izquierdo-Barba, M. Manzano, *Molecules* **2017**, *23*, 47.

[25] Z. Gounani, M. A. Asadollahi, J. N. Pedersen, J. Lyngsø, J. Skov Pedersen, A. Arpanaei, R. L. Meyer, *Colloids Surfaces B Biointerfaces* **2019**, *175*, 498.

[26] S. Jiang, Y. Zhang, Y. Shu, Z. Wu, W. Cao, W. Huang, *Biomed. Mater.* **2017**, *12*, 25017.

[27] S.-W. Song, K. Hidajat, S. Kawi, *Langmuir* **2005**, *21*, 9568.

[28] J. Rivadeneira, G. M. Luz, M. C. Audisio, J. F. Mano, A. Alejandro, **2015**, 128.

[29] D. Massiot, F. Fayon, M. Capron, I. King, S. Le Calvé, B. Alonso, J.-O. Durand, B. Bujoli, Z. Gan, G. Hoatson, *Magn. Reson. Chem.* **2002**, *40*, 70.

[30] T. Kokubo, H. Kushitani, S. Sakka, T. Kitsugi, T. Yamamuro, *J. Biomed. Mater. Res.* **1990**, *24*, 721.

[31] D. M. Pickup, P. Guerry, R. M. Moss, J. C. Knowles, M. E. Smith, R. J. Newport, *J. Mater. Chem.* **2007**, *17*, 4777.

[32] M. Al Qaysi, N. J. Walters, F. Foroutan, G. J. Owens, H. W. Kim, R. Shah, J. C. Knowles, *J. Biomater. Appl.* **2015**.

[33] F. Zhang, Y. Yan, H. Yang, Y. Meng, C. Yu, B. Tu, D. Zhao, *J. Phys. Chem. B* **2005**,

109, 8723.

[34] A. Vinu, *Adv. Funct. Mater.* **2008**, *18*, 816.

[35] F. Foroutan, N. J. Walters, G. J. Owens, N. J. Mordan, H.-W. Kim, N. H. de Leeuw, J. C. Knowles, *Biomed. Mater.* **2015**.

[36] E. A. Abou Neel, J. C. Knowles, *J. Mater. Sci. Med.* **2008**, *19*, 377.

[37] N. Eliaz, N. Metoki, *Materials (Basel).* **2017**, *10*, 2.

[38] D. Durgalakshmi, R. A. Rakkesh, S. Balakumar, *Appl. Surf. Sci.* **2015**, *349*, 561.

[39] N. Cheng, Y. Wang, Y. Zhang, B. Shi, *PLoS One* **2013**, *8*, 1.

[40] K. S. Rana, L. P. De Souza, M. A. Isaacs, F. N. S. Raja, A. P. Morrell, R. A. Martin, *ACS Biomater. Sci. Eng.* **2017**, *3*, 3425.

[41] L. Zhao, X. Yan, X. Zhou, L. Zhou, H. Wang, J. Tang, C. Yu, *Microporous Mesoporous Mater.* **2008**, *109*, 210.